Short Range Order in Liquid Lithium-Sodium Alloys

Henner Ruppersberg

Angewandte Physik, Universität des Saarlandes, Saarbrücken

Walter Knoll

Institut Laue-Langevin, Grenoble

(Z. Naturforsch. **32 a**, 1374–1382 [1977]; received September 13, 1977)

The short range order of a liquid lithium sodium alloy with nearly critical composition has been studied by small-angle and high-angle neutron diffraction at 10 and 145 K above the critical temperature. In this temperature range the small-angle scattering yields linear Ornstein-Zernike plots from which formally critical exponents and amplitudes could be determined. The atoms prefer like nearest neighbors and the extent of this preference varies only slowly with temperature.

Introduction

Because of the negative coherent neutron scattering amplitude of the Li^7 isotope, lithium alloys are ideal candidates for the study of short-range order (SRO) by neutron diffraction. Most nuclides have a positive scattering amplitude, and if one of them is mixed with Li^7 at the so-called zero alloy composition the coherent scattering pattern directly reveals the amplitude of concentration-fluctuation waves. In previous papers [1, 2] the SRO of liquid LiPb and LiAg alloys has been investigated. The general physical and chemical behavior of LiPb and LiAg alloys is typical for system with strong and medium tendency, respectively, towards compound formation. For both systems a quite similar preference for unlike nearest neighbors has been observed. From preliminary results [3] we have the impression that the stronger bonding of LiPb in the vicinity of the composition Li_4Pb is manifested in a larger range of the SRO.

In this paper the SRO and its temperature variation of the segregating system LiNa is studied. In segregation systems, long-wavelength fluctuations yield strong scattering effects at small wave vectors, and in addition to the usual high-angle scattering experiments special small-angle scattering investigations with another instrument become necessary. Because the angular ranges of the two experiments did not overlap, the small-angle region was extrapolated by means of an Ornstein-Zernike (OZ) plot, and the gap was closed by a smooth interpolation.

Reprint requests to Prof. Dr. H. Ruppersberg, Angewandte Physik, Universität des Saarlandes, *D-6600 Saarbrücken 11*.

The sodium lithium phase diagram is dominated by a region of two immiscible liquids. The composition and temperature coordinates, x and T, of the immiscibility loop have since 1968 been determined by Kanda et al.[4] by means of density measurements and by Schürmann and Parks [5], by Down et al. [6] and by Feitsma et al. [7] from the temperature and composition dependence of the electrical resistivity R. The results obtained by the different authors agree very well. The consolute point occurs at $x_{Li}^c = 64 \pm 2$ at.% and $T_c = 577 \pm 2$ K. This is 138 and 76 K below that reported before 1960 by Howland and Epstein [8] and Salmon and Ahmann [9], respectively. Feitsma et al.[7] calculated a 583 K isotherm of $R(x)$ by substituting partial structure factors based on the hard sphere solution of the Percus-Yevick equation in the resistivity formula of Faber and Ziman. The packing fractions were linearly interpolated between $\eta_{Na} = 0.397$ and $\eta_{Li} = 0.404$. The results of the calculations depend very strongly on the value of the hard sphere diameter chosen for lithium. The value $\sigma_{Li} = 2.43$ Å together which $\sigma_{Na} = 3.26$ Å gave satisfactory quantitative agreement with experiment. According to Schürmann and Parks [5] the effects of the order parameter fluctuations on the resistivity itself are surprisingly small, but dR/dT rises if the miscibility loop is approached from higher temperatures, and it has a sharp peak at the critical point. This behavior, which the authors call "paraconductivity", cannot be derived from the long-wavelength fluctuations which are related to the small-angle scattering, and on the basis of the discussion by Fisher and Langer [10] it is expected to be due to short-wavelength fluctuations. No direct experimental information about the amount and the temperature variation of such fluctuations in liquid

alloys has been available until now. Small angle scattering experiments were performed with X-rays by Brumberger et al[11]. From an OZ plot, the authors calculated the long-range correlation length and its temperature dependence as well as the temperature variation of the logarithm of the concentration fluctuations $\lg(N\langle\Delta x^2\rangle)$. They observed a critical temperature of $T_c = 580.16$ K. In this work the complete distance-correlation function of concentration fluctuations and its temperature dependence is calculated from small- and high-angle neutron diffraction data.

Theory

For homogeneous binary substances made from atoms A and B the total structure factor $S(k)$ which results from a scattering experiment may be broken down into a weighted sum of three partial structure factors. In terms of the number concentration structure factors, which have been introduced by Bhatia and Thornton[12], $S(k)$ is given by

$$S(k) = [\langle b\rangle^2 S_{NN} + 2\langle b\rangle \Delta b\, S_{NC} + \Delta b^2 S_{CC}]/\langle b^2\rangle , \quad (1)$$

$k = 4\pi \sin\Theta/\lambda$, 2Θ is the scattering angle and λ the wavelength. b_A is the coherent scattering amplitude of pure A, $\Delta b = b_A - b_B$, $\langle b\rangle = x_A b_A + x_B b_B$. $S(k)$ is normalized to approach 1 at high scattering angles. The same is true for $S_{NN}(k)$. The Fourier transform of $(S_{NN}-1)$ is a measure of the distance correlation of local A and B atom number – density fluctuations. Thus, $S_{NN}(k)$ describes the overall structure and it has the same signification as the structure factor of a monoatomic substance. $S_{NN}(k)$ becomes equal to the structure factor of pure A in the limit of $x_A = 1$. $S_{NC}(k)$ oscillates around zero. Its Fourier transform describes the cross-correlation between density and concentration fluctuations. The term containing $S_{CC}(k)$ is equal to $x_A x_B$ if the mutual distribution of A and B atoms is random. From $S_{CC}(k)$ the "radial concentration correlation function" (RCF) $4\pi r^2 \varrho_{CC}(r)$ which has been introduced by Ruppersberg and Egger[1], is calculated according to

$$4\pi r^2 \varrho_{CC}(r) = \frac{2r}{\pi}\int k\,[S_{CC}(k)/x_A x_B - 1] \cdot \sin k r\, dk . \quad (2)$$

This curve is negative for distances with preference for unlike pairs and positive for like pairs. From this curve the Warren short-range order parameters are calculated in the case of polycrystalline disordered alloys. $S_{CC}(0)$ is proportional to the extent of concentration fluctuations:

$$RT/S_{CC}(0) = RT/(N\langle\Delta x^2\rangle) = \partial^2 G/\partial x^2 = E^{xs} + RT/x_A x_B \quad (3)$$

G is the Gibbs free energy, $E^{xs} = -2RT\,\partial \ln \beta_A/\partial x_B^2$ is the "excess stability function" which has been introduced by Darken[13], β is the activity coefficient. R and T have their usual meaning. A tendency towards compound formation is indicated by positive values of E^{xs}. $S_{CC}(0)$ is then smaller than $x_A x_B$ and in the few cases studied until now, $S_{CC}(k)$ exhibits a first positive peak at about $k = 1.7$ Å^{-1}, followed by several rapidly damped oscillations[1]. In these cases the RCF is negative at the distance of nearest neighbors and beyond this distance it exhibits oscillations around zero which seem to be damped the more rapidly the smaller the above mentioned first peak of $S_{CC}(k)$ is[3]. Negative values of E^{xs} indicate a tendency towards segregation. At the critical point $\partial^2 G/\partial x^2$ becomes zero and $S_{CC}(0)$ diverges. Near the critical point $S_{CC}(0)$ varies with temperature according to

$$S_{CC}(0) = K T \varepsilon^{-\gamma} \quad \text{and}$$

$$\frac{\partial}{\partial T}(\partial^2 G/\partial x^2) = (R\gamma/K T_c)\,\varepsilon^{\gamma-1} \quad (4)$$

$\varepsilon = (T - T_c)/T_c$, and the limit of γ for $\varepsilon \to 0$ is called[14] the critical-point exponent of $S_{CC}(0)$. According to the Ornstein-Zernike theory in the small angle region $S_{CC}(k)$ is given by

$$S_{CC}^{OZ}(k) = S_{CC}(0)/(1 + \xi^2 k^2) . \quad (5)$$

ξ is called correlation length and its temperature dependence is given by

$$\xi = \xi_0 \varepsilon^{-\nu} . \quad (6)$$

The limiting value of ν is the critical exponent of the correlation length. Classical theories predict $\gamma = 1$ and $\nu = 0.5$, whereas lattice-gas predictions are $\gamma = 1.25$ and $\nu = 0.643$. The RCF which results from Eq. (2) if for $S_{CC}(k)$ at all k the expression (5) is inserted is given by

$$4\pi r^2 \varrho_{CC}^{OZ}(r) = r\, S_{CC}(0) \cdot (x_A x_B)^{-1} \xi^{-2} \cdot e^{-r/\xi} . \quad (7)$$

This curve is zero for $r = 0$, it then rises to a maximum value at $r = \xi$ and decreases again, but it always remains positive. Thus, it shows a wrong behavior at small r, where $\varrho_{CC}(r)$ is zero for distances smaller than the hard sphere diameter of the smallest atoms, and also at large r where the true $\varrho_{CC}(r)$ should change its sign or should exhibit

oscillations around zero, because necessarily there will be an excess of AB pairs for larger r values if there is an excess of AA and BB pairs at small distances. The deviations of $\varrho_{CC}^{OZ}(r)$ from the correct behavior are reflected in the high-angle part of $S_{CC}(k)$. In general it is quite problematical, if not impossible, to separate this high angle portion from a measured $S(k)$ curve. Only in the case of a so-called "zero-alloy", for which $\langle b \rangle = 0$ and $x_A = b_B/(b_B - b_A)$, according to Eq. (1), $S_{CC}(k)$ can directly be measured. The zero alloy composition of Li^7 combined with natural Na is at about $x_{Li} = 0.61$ which is quite near to the critical composition.

Experimental

The samples were prepared in a glove box from 99.9% sodium and from lithium containing 99.05% Li^7 and 0.95% Li^6. They were filled into cylindrical vanadium containers and sealed by electron beam welding. The containers were made by the Institut für Kernphysik, Stuttgart from 0.1 mm vanadium foil and had an external diameter of 11.4 mm.

The neutron diffraction experiments were carried out at the D4 and D11 instruments of the Institut Laue-Langevin, Grenoble, France. Detailed instrument description are published by this institute [15]. In the D4 machine the samples were held in a vertical cylindrical resistivity furnace. The irradiated volume of the samples was defined to better than 0.3% by boron nitride screens. The heating element consisted of a thin walled (0.1 mm) vanadium cylinder of 20.5 mm inner diameter with top and bottom made from stainless steel. The heating element was screwed on a ground plate at which the sample was fixed on the top of an isolating column and which was centered in the vacuum vessel of the goniometer. The heating element was filled with helium at atmospheric pressure. The vacuum tightness of the system was achieved by means of a temperature resistant metallic 0-ring. The temperature of the sample was measured with a Chromel-Alumel thermocouple and it was controlled to better than ± 1 K by a PID thyristor controller.

The primary beam had a wavelength of 0.696 Å and in the region of the sample it had a height of 50 mm and a width of 15 mm. The scattered neutrons were detected by a He^3 counter which was placed at 1400 mm from the center of the goniometer. The receiving slit was 50 mm high and 20 mm large. Intensities were measured in an angular range corresponding to $0.19 \leqq k \leqq 10$ Å^{-1}. The intensities from the sample were corrected for background scattering, absorption, and inelastic effects, and they were normalized in almost the same way as described by Ruppersberg and Egger [1]. The Paalman and Pings absorption factors were substituted by values calculated according to Poncet [16] which take properly into account the existence of the cylindrical heating element. In order to correct for masking effects of the sample which are important at small angles, as has been shown by Bertagnolli et al. [17], an additional run with a cadmium rod replacing the sample was performed. The correction procedure has been checked using a vanadium sample for which even at k values smaller than 0.5 Å^{-1} a flat signal was obtained. The D4 machine is designed to measure with high efficiency the broad diffraction patterns of amorphous substances and has a poor angular resolution especially at small angles. Because for the present study the knowledge of the exact profile of the small angle scattering peak is important the measured intensities had to be corrected for the unsymmetrical and angle-dependent broadening effects. The corresponding deconvolution was performed following the method of van Cittert [18] which has been studied recently by Wertheim [19]. In Fig. 1 the small-angle parts of an original and of a deconvoluted D4 curve are shown and it can be observed that the resolution correction does not change drastically the shape of $S(k)$. At higher angles it significantly sharpens the first peak of the measured structure factor, the amplitude of which rises in the case of liquid sodium, e. g., from 2.9 to 3.0, and the flank at the low angle side becomes steeper. The D4

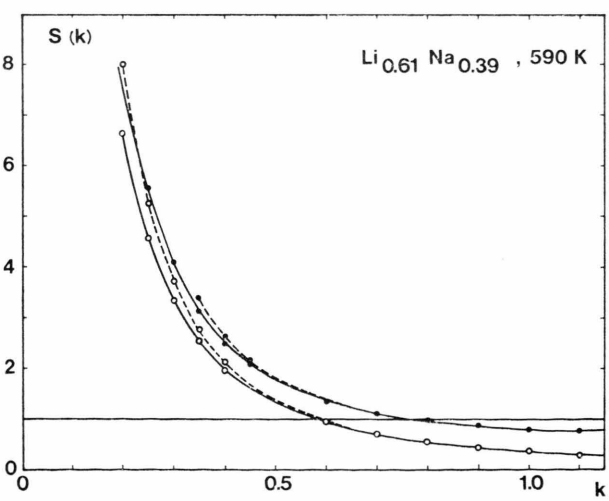

Fig. 1. Influence of the D4 instrumental broadening, demonstrated for results obtained at 590 K: *Full line with points:* original D4 data. *Broken line with points:* defolded D4 data. *Full line with circles:* OZ curve calculated from critical coefficients and folded. *Broken line with circles:* calculated from critical coefficients.

instrument is extremely sensitive for the detection of small angle scattering. But in the k-range accessible with this instrument, the scattered intensity is very insensitive to variations of critical amplitudes and exponents. Because these data have to be known for the calculation of short-range order, the same zero alloy sample which has been studied on the D4 machine was investigated with the small-angle scattering instrument D11.

To measure the small-angle scattering with the D11 instrument a monochromatic neutron beam of 6.7 Å wavelength was used with a height of 10 mm and a width of 2 mm. The scattered intensity was detected by a flat multicounter containing 4096 cells in an area of (640×640) mm^2. The distance between sample and container was 2370 mm, thus giving an accessible k-range of $0.04 \leqq k \leqq 0.14$ Å^{-1}. The sample was placed in a cylindrical conduction-type furnace. Two copper blocks in thermal contact with the top and the bottom of the sample were held at the same temperature with a stability of ± 0.5 K. The whole assembly was centered in a He-filled quartz tube of 30 mm inner diameter. The diffraction pattern of the sample was corrected in the usual way for absorption and background scattering and normalized by means of an additional vanadium run.

Because no facilities are provided to stir the samples, neither in the D4 nor in the D11 furnace, prior to a measurement the alloys were held at about 150 K above T_c for a sufficiently long period. In the high-angle range, after about eight hours the counting rates became constant, whereas we had to wait twelve hours in the small angle region. With the D4 machine we then obtained reproducible data over five days. Once the sample homogenized, after a temperature variation above T_c the new equilibrium was reached almost instantaneously.

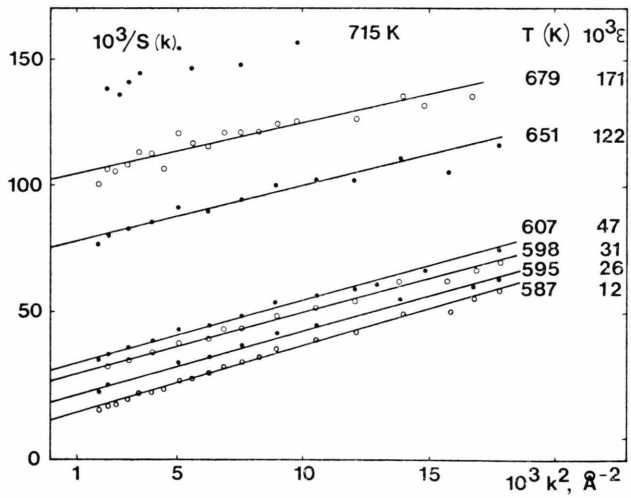

Fig. 2. Ornstein-Zernike plots of the small-angle scattering patterns of liquid $Li_{0.61}Na_{0.39}$ obtained with the D11 instrument.

Results

From the OZ-plot of the small angle scattering patterns, Fig. 2, $S_{CC}(0)$ and ξ are calculated according to Equation (5). In Fig. 3 is depicted a plot of $\lg \xi$ and $\lg T/S(0)$ against $\lg \varepsilon$. Least square fits yield the coefficients of Eqs. (4) and (6) and we obtain $\xi = 1.7\,\varepsilon^{-0.57}$ and $S_{CC}(0) = 5 \cdot 10^{-4}\, T\, \varepsilon^{-1.1}$.

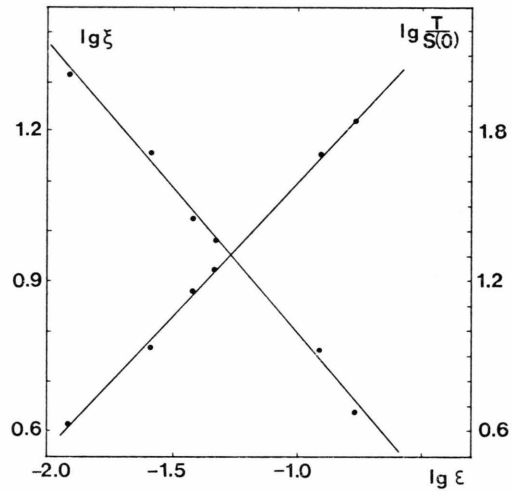

Fig. 3. Plots of $\lg \xi$ and $\lg[T/S(0)]$ against $\lg \varepsilon$, according to Eqs. (4) and (6).

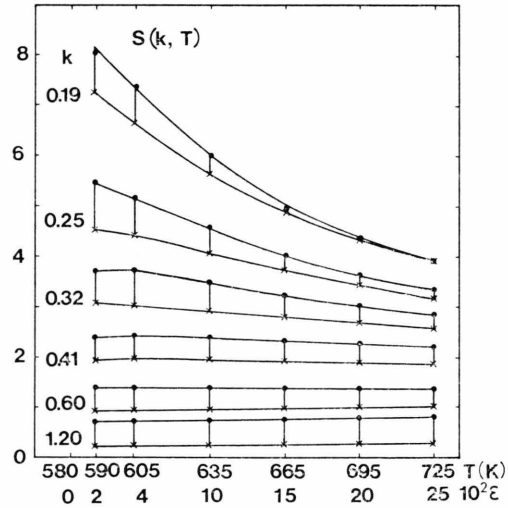

Fig. 4. Comparison of $S(k, T)$ data obtained with the D4 instrument (points), with curves (crosses) calculated from the critical exponents and amplitudes and which have been folded with the resolution function of the D4 instrument.

The D11 curves yield a critical temperature of about 580 K and at the same temperature at small angles a discontinuity of the intensity versus temperature curves of the D4 instrument has been observed. In Fig. 4 the variation of $S(k)$ with temperature is shown for several k-values beyond the small angle region. In the graph the experimental D4-data (points) are compared with extrapolated D11 data (crosses) which have been folded with the resolution function of the D4 instrument. The two sets of data have been obtained with different instruments, wavelength and normalization procedures and the deviations between corresponding curves cannot be assumed to be significant, though it seems plausible that in this k-range the $S_{CC}(k)$ values are already larger than those obtained from the OZ curves. The influence of the folding on an OZ-curve is demonstrated in Figure 1.

The total $S(k)$ curves for Li, Na and for three alloys, obtained from the defolded D4 data, are shown in Figure 5. The oscillations of the alloy curves beyond the small angle scattering region are extremely small, especially in the case of the zero alloy, and could hardly be detected. Extremely large counting rates and repeated runs with two different samples proved them to be significant. To make these small oscillations visible the amplitudes of the $S(k)$ curves of the alloys, Fig. 5, have been enlarged by a factor of ten at high k values. These curves are shown as broken lines. The Na-curve is very similar to the curve obtained by Greenfield and Wiser [20] by X-ray diffraction. The Li-curve is similar to that calculated theoretically by Jacucci et al. [21].

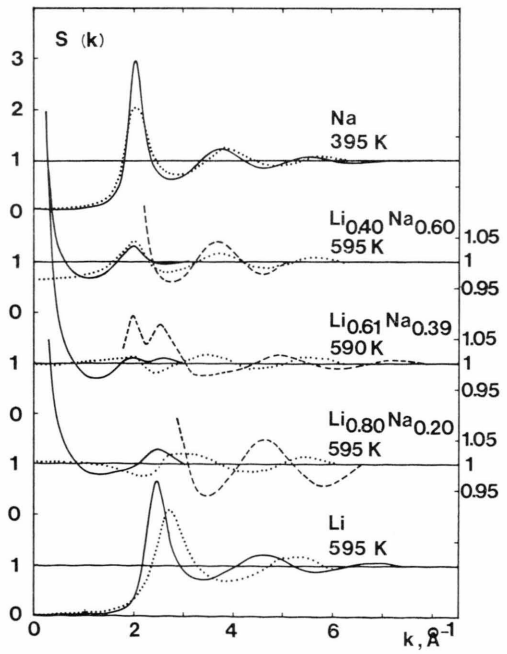

Fig. 5. Total structure factors of lithium, sodium and of three LiNa alloys calculated from the D4 data corrected for instrumental broadening. Full lines: left hand scale, broken lines: right hand scale. Points: $S(k)$ calculated from the PY-hard sphere equation with the parameters published by Feitsma et al. [7].

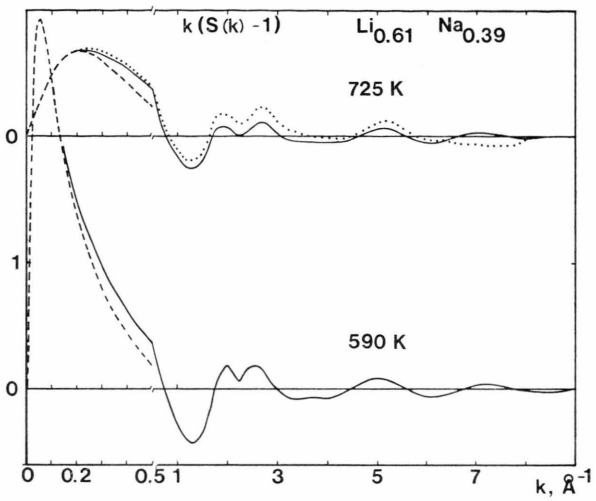

Fig. 6. $k[S(k)-1]$ curves of the liquid zero alloy $Li_{0.61}Na_{0.39}$ at 10 K and 145 K above the critical temperature. The k-scale is expanded at $k<0.5$. *Broken lines:* calculated OZ-curves. *Full lines:* calculated from defolded D4 data with smooth interpolation between D4 and OZ data at low k values. The curves are corrected to eliminate the spurious ripples at small r in the $4\pi r^2 \varrho_{CC}(r)$ curves of Figure 8. *Points:* original D4 data, yielding ripples at small r in the Fourier transform, Figure 8.

$k[S(k)-1]$ curves of the zero alloy are depicted in Fig. 6 for 725 and 590 K. The k-scale is changed at $k=0.5$. The broken-line curves are calculated from the small-angle scattering. A smooth line has been drawn between the high- and small-angle scattering regions. The points of the 725 K curve have been obtained in a straightforward way from the experimental data. But the RCF calculated from this curve, which is shown in Fig. 8, exhibits spurious ripples at small r-values which disappear without altering the curve beyond 2.5 Å, if the points are transformed into the full-line curve. The corresponding variation of the original data is within the error limits of the measurements and the normalization procedure. For 590 K only the corrected $k[S(k)-1]$ curve is shown. The ripples of the RCF are somewhat smaller than those observed at 725 K.

Tentative D4 runs with an alloy of 65% Li, which is near to the critical composition, yielded almost the same results as the zero-alloy.

Discussion

From the small-angle scattering experiments in the range of $0.012 \leqq \varepsilon \leqq 0.17$ we obtain critical exponents of $\gamma = 1.1$ and $\nu = 0.57$. These values are smaller than those published by Wu and Brumberger [11] who observed in a temperature range corresponding to $10^{-4} < \varepsilon < 10^{-2}$ values of 1.296 ± 0.061 and 0.655 ± 0.03 for γ and ν, respectively. This discrepancy might be due to the fact that the critical-point exponents are the limiting values of γ and ν for $\varepsilon = 0$, and it is known [14] that at higher temperatures the behavior of the system corresponds more to the classical mean field case with $\gamma = 1$ and $\nu = 0.5$.

At temperatures which correspond to ε larger than 0.17, the intensity of the D11 curves becomes too small to allow further demonstration of the validity of Eq. (5), see Figure 2. But we suppose that the exponents and amplitudes which result from the plots of Fig. 3 are still valid at 725 K, or $\varepsilon = 0.25$, to describe the small angle part of the corresponding D4 measurement, which is shown in Figure 6. Because experimental thermodynamic data of LiNa alloys do not exist and because a calculation of these data from the phase diagram is too inaccurate [22], we are unable to verify directly the value of $5 \cdot 10^{-4}$ which we obtained for K, Equation (4). However, Ansara [22] calculated $(\partial^2 G/\partial x^2)$ curves for several liquid alloys with miscibility gap. For temperatures above the consolute point he observed an almost linear variation of this quantity with temperature. The corresponding slopes are 6.0, 6.5 and 7.0 cal/K for Hg/Ga, Hg/Na and Ga/Pb, respectively. According to the classical theory $\gamma = 1$, and from Eq. (4) a linear variation of $(\partial^2 G/\partial x^2)$ with temperature results. In our case $\gamma = 1.1$, and the slope is zero at T_c. But about 40 K beyond this temperature the curve becomes almost linear, and at $T_c + 100$ K the slope is 6.4; the mean slope between T_c and $T_c + 100$ K is 5.8 cal/K, and these values correspond very well with those observed for the other systems mentioned above. The value of 1.7 Å which we observed for ξ_0 is within the error limits of the X-ray result [11] of 1.56 ± 0.21 Å.

According to Schürmann and Parks [5] the behavior of $S_{CC}(k)$ beyond the small angle scattering region should explain the phenomenon of paraconductivity. The electrical resistivity R is related to the structure via the Faber-Ziman equation:

$$R \cong \int_0^1 (k/2\,k_f)^3 \,[\langle u\rangle^2 S_{NN}(k) + 2\langle u\rangle \Delta u\, S_{NC}(k) + (\Delta u)^2 S_{CC}(k)]\, d(k/2\,k_f)\,. \qquad (8)$$

$k_f = 0.97$ Å^{-1} is the Fermi momentum, u_A is the pseudopotential formfactor of the species A. The $\langle\ \rangle$ and Δ symbols have the same signification as in Equation (1). The paraconductivity should be related to the temperature variation of $S_{CC}(k)$ at k between k_f and $2k_f$. But, because nothing special can be observed from this function shown in Figs. 4 and 5, we studied the question of whether already the $S_{CC}^{OZ}(k)$ term could be responsible for the divergence of (dR/dT) at T_c. In Fig. 7, $k^3[dS_{CC}^{OZ}(k)/dT]$ is plotted for different ε values as a function of $\log k$. These curves have been calculated from the temperature derivatives of Eqs. (4) to (6) by inserting for ξ_0 and the critical exponents the values published by Wu and Brumberger [11] (broken lines) and our data (full lines). In both cases K, Eq. (4), was supposed to be $5 \cdot 10^{-4}$. At small k values, where the pseudo-potential form-factors are small, the curves

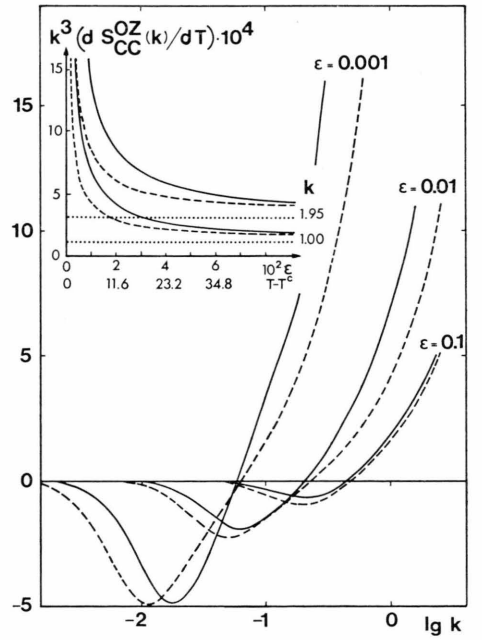

Fig. 7. Plots of $k^3[\partial S_{CC}^{OZ}(k)/\partial T]$ versus $\lg(k)$ for different ε-values, and versus ε for different k-values. *Full lines:* $\gamma = 1.1$, $\nu = 0.57$, $K = 5 \cdot 10^{-4}$, $\xi_0 = 1.7$. *Broken lines:* $\gamma = 1.296$, $\nu = 0.655$, $K = 5 \cdot 10^{-4}$, $\xi_0 = 1.56$. *Points:* $\gamma = 1.0$, $\nu = 0.5$, $K = 5 \cdot 10^{-4}$, $\xi_0 = 1.7$.

are negative, but for short-wavelength fluctuations they become positive. The k-value beyond which the curves are positive decreases and their ordinate values increase if T diminishes and approaches T_c. In Fig. 7 are also plotted several curves $k^3(\mathrm{d}S_{CC}^{OZ}/\mathrm{d}T)$ versus ε at $k=1$ and 1.95 Å^{-1}. In this figure two additional curves (points) are shown which were calculated from the classical critical parameters and with $\xi_0=1.7$ and $K=5\cdot10^{-4}$. The classical curves are almost invariant with T down to extremely small ε-values, and for liquid alloys following the classical law no paraconductivity should be observed. The other curves of Fig. 7 show almost exactly the behavior of the $(\mathrm{d}R/\mathrm{d}T)$ curves published by Schürmann and Parks [5]. Paraconductivity will not be observed if the pseudopotential form-factors of the two species are identical because then the term with S_{CC} in Eq. (8) will vanish. A theoretical discussion of the behavior of the electrical resistivity at phase transitions in binary alloys is presented by Binder and Stauffer [23] on the basis of a structure factor proposed by Fisher and Aharony [24] for $k\xi \gg 1$.

The hard sphere curves calculated from the η and σ data proposed by Feitsma et al. [7] are plotted in Fig. 5 together with the measured curves, and they are seen to be very different from the experimental data. For the pure constituents a better agreement is obtained if both η_{Na} and σ_{Li} are enlarged. The problems involved with the hard sphere description of the structure factor of liquid sodium have extensively been discussed by Greenfield et al [25]. We tried to calculate $S_{CC}(k)$ of the zero alloy with a large variety of η and σ_{Li}/σ_{Na} values, but we never obtained a curve similar to the experimental one, with peaks at 2 and 2.5 Å^{-1}. This double peak obviously is due to a special structure of the melt, and a comparison with the other curves of Fig. 5 suggests that it is due to preferred LiLi distances in Li rich clusters and to corresponding Na distances. The question of how it is possible that characteristic parts of the S_{NN}-structure factors are visible in the S_{CC} function will be explained below.

As has been shown by Hargrove [26] for systems with a tendency towards segregation, the oscillations of $S_{CC}(k)$ beyond the small angle scattering region are extremely small. Correspondingly, the $\varrho_{CC}(r)$ curves, Fig. 8, are quite similar to the $\varrho_{CC}^{OZ}(r)$ curves, already for next-nearest neighbors. The same has been observed by Binder and Rauch [27] for Heisenberg ferromagnets by means of computer simulation

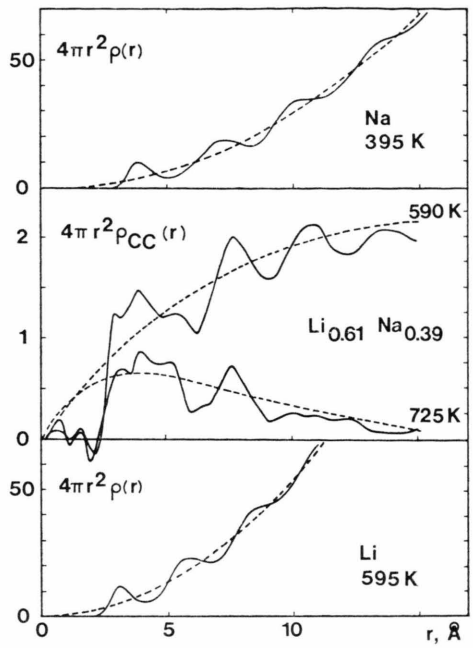

Fig. 8. Radial distribution functions of pure liquid Li and Na, radial concentration-fluctuations correlation functions (RCF) of the liquid zero-alloy $Li_{0.61}Na_{0.39}$. The *broken lines* are $4\pi r^2\varrho_0$-curves and $4\pi r^2\varrho_{CC}^{OZ}(r)$ curves, respectively.

experiments. At small distances the difference between the OZ- and the measured curves, Fig. 8, seems just to be due to the finite size of the atoms. A comparison with the radial distribution function of the pure constituents, which are shown in the same figure, demonstrates that the peaks at 3 and 4 Å are due to preferred LiLi and NaNa distances. In order to calculate approximate values of the Warren short-range order parameter α_1, we separated a gaussian shaped peak at 3 Å from the rest of the curve. Assuming that each atom has ten nearest neighbors, from the area of this peak α_1 values of 0.5 and 0.3 result for 590 and 725 K, respectively. These very approximate values indicate that Li atoms have 8 and 7 Li atoms as nearest neighbors instead of 6 in the case of a random distribution. If the temperature approaches T_c, in the classical case the RCF^{OZ} at 3 Å rises from 0.97 at 590 K to 1.12 at 581 K and to 1.20 at $T_c=580$ K. At the same distance but for the critical coefficients $\nu=0.57$ and $\gamma=1.1$ observed in this paper it rises from 0.87 at 590 K to a maximum value of 0.90 at 583 K and then decreases again. From the coefficients observed by Wu and Brumberger [11], a value of 1.20 is

calculated for 590 K which increases to 1.27 at 580.7 K, i. e. at $\varepsilon = 10^{-3}$, and then decreases. But, because according to Fisher and Burford [28] the OZ formalism does not apply to very small ε values, the calculated decrease of the RCF^{OZ} in the vicinity of T_c is not correct. Thus, the nearest neighbor arrangement in liquid LiNa varies only very slowly with temperature. In the temperature range between T_c and $T_c + 145$ K the SRO parameter is only reduced by a factor of about 0.5. The quantities which vary strongly with temperature are the SRO parameters at large distance and the correlation length. At large distances, where the oscillations of the RCF and of the global radial distribution function are small, the SRO parameters are given by $\alpha = 4\pi r^2 \varrho_{CC}(r)/4\pi r^2 \varrho_0$, where ϱ_0 is the mean number density. At 590 K for $r = \xi$ a value of $\alpha = 0.02$ results. A temperature rise of 135 K reduces α at the same r value to $6 \cdot 10^{-4}$. From Fig. 9 it can be observed that α becomes negative only for distances larger than about seven times the correlation length.

In terms of the partial pair correlation functions, $\varrho_{ij}(r)$, $(i, j = A, B)$, the RCF is given by

$$4\pi r^2 \varrho_{CC}(r) = x_B 4\pi r^2 (\varrho_{AA} + \varrho_{AB}) + x_A 4\pi r^2 \cdot (\varrho_{BB} + \varrho_{BA}) - \frac{1}{x_A} 4\pi r^2 \varrho_{BA}. \quad (9)$$

$\varrho_{ij}(r)$ is the mean number of j-type atoms per unit volume at the distance r from an i-type atom. In the extreme case of concentration fluctuations which yield droplets of pure A and B, $\varrho_{AB}(r)$ is negligible at sufficiently small r-values, and the RCF is composed of the weighted sum of the radial distribution functions of pure A and B and it oscillates around $4\pi x_A x_B r^2 \varrho_0$. Due to the finite size of the droplets, with increasing r the RCF will fall below $4\pi x_A x_B r^2 \varrho_0$ and at sufficiently large r-values, the RCF will oscillate around zero. $S_{CC}(k)$ is calculated from the RCF by inversing Eq. (2) and it will contain elements of the structure factors of pure A and B, and in addition some small angle scattering due to the finite size of the doplets. This explains why in the zero-alloy curves of Figs. 5 and 8 characteristic parts of the S_{NN} structure factor of the pure constituents are visible.

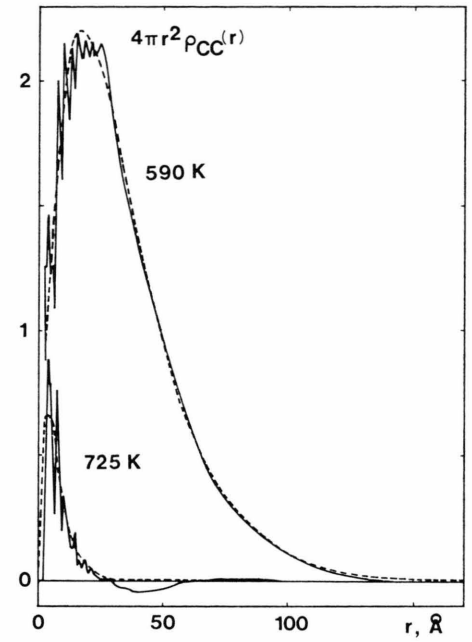

Fig. 9. Radial concentration-fluctuation correlation functions (RCF) of the liquid zero-alloy $Li_{0.61}Na_{0.39}$ at 10 K and 145 K above the critical temperature. *Broken lines:* RCF^{OZ} curves.

Acknowledgements

The authors gratefully acknowledge financial support of the Deutsche Forschungsgemeinschaft and of the Institut Max von Laue – Paul Langevin. Thanks are due to Professor K. Binder and to Dr. I. Ansara for helpful discussions.

[1] H. Ruppersberg and H. Egger, J. Chem. Phys. **63,** 4095 [1975].
[2] H. Reiter, H. Ruppersberg, and W. Speicher, Inst. Phys. Conf. Ser. **30,** 133 [1977].
[3] H. Ruppersberg and H. Reiter, Ber. Bunsenges. (in press).
[4] F. A. Kanda, R. C. Faxon, and D. V. Keller, J. Phys. and Chem. Liquids **1,** 61 [1968].
[5] H. K. Schürmann and R. D. Parks, Phys. Rev. Lett. **27,** 1790 [1971].
[6] M. G. Down, P. Hubberstey, and R. J. Pulham, J. C. S. Dalton, 1490 [1975].
[7] P. D. Feitsma, J. J. Hallers, F. V. D. Werf, and W. van der Lugt, Physica **79 B,** 35 [1975].
[8] W. H. Howland and L. F. Epstein, Adv. Chem. Ser. **19,** 34 [1957].
[9] O. N. Salmon and D. H. Ahman, J. Phys. Chem. **60,** 13 [1956].
[10] M. E. Fisher and S. L. Langer, Phys. Rev. Lett. **20,** 665 [1968].
[11] H. Brumberger, N. G. Alexandropoulos, and W. Claffey, Phys. Rev. Lett. **19,** 555 [1967]. E. S. Wu and H. Brumberger, Phys. Lett. **53 A,** 475 [1975].
[12] A. B. Bhatia and D. E. Thornton, Phys. Rev. **B 2,** 3004 [1970].
[13] L. S. Darken, Trans. AIME **239,** 80 [1967].

[14] H. E. Stanley, Introduction to Phase Transitions and Critical Phenomena, Clarendon Press, Oxford 1971.
[15] ILL Neutron Beam Facilities, available from ILL, 156X, Centre de Tri, 38042 Grenoble-Cedex, France.
[16] P. F. J. Poncet, Thesis, University of Reading, U.K. 1976.
[17] H. Bertagnolli, P. Chieux, and M. D. Zeidler, Molec. Phys. **32,** 759 [1976].
[18] P. H. van Cittert, Z. Phys. **69,** 298 [1931].
[19] G. H. Wertheim, J. Electron, Spect. Rel. Phen. **6,** 239 [1975].
[20] A. J. Greenfield and N. Wiser, Phys. Lett. **34 A,** 123 [1971]; A. J. Greenfield, J. Wellendorf, and N. Wiser, Phys. Rev. **A 4,** 123 [1971].
[21] G. Jacucci, M. L. Klein, and R. Taylor, Solid State Comm. **19,** 657 [1976].
[22] I. Ansara, private communication.
[23] K. Binder and D. Stauffer, Z. Phys. **B 24,** 407 [1976].
[24] M. E. Fisher and A. Aharony, Phys. Rev. **B 10,** 2818 [1974].
[25] A. J. Greenfield, N. Wiser, M. R. Leenstra, and W. van der Lugt, Physica **59,** 571 [1972].
[26] W. H. Hargrove, Thesis, University of Alberta, Canada 1976.
[27] K. Binder and H. Rauch, Z. Phys. **219,** 201 [1969].
[28] M. E. Fisher and R. J. Burford, Phys. Rev. **156,** 583 [1967].